

See discussions, stats, and author profiles for this publication at: <https://www.researchgate.net/publication/44631732>

On-Chip Immunoassay Using Surface-Enhanced Raman Scattering of Hollow Gold Nanospheres

ARTICLE *in* ANALYTICAL CHEMISTRY · JUNE 2010

Impact Factor: 5.64 · DOI: 10.1021/ac100736t · Source: PubMed

CITATIONS

74

READS

19

8 AUTHORS, INCLUDING:



Hyangah Chon

Hanyang University

17 PUBLICATIONS 646 CITATIONS

SEE PROFILE



Soo-Ik Chang

Chungbuk National University

91 PUBLICATIONS 1,655 CITATIONS

SEE PROFILE



Jaebum Choo

Hanyang University

207 PUBLICATIONS 4,929 CITATIONS

SEE PROFILE

On-Chip Immunoassay Using Surface-Enhanced Raman Scattering of Hollow Gold Nanospheres

Hyangah Chon,[†] Chaesung Lim,[†] Seung-Mo Ha,[‡] Yoomin Ahn,[‡] Eun Kyu Lee,[§] Soo-Ik Chang,[‡] Gi Hun Seong,[†] and Jaebum Choo^{*,†}

Departments of Bionano Engineering and Mechanical Engineering, Hanyang University, Ansan 426-791, South Korea, College of Bionanotechnology, Kyungwon University, Sunnam 461-701, South Korea, and Department of Biochemistry, Chungbuk National University, Cheongju 361-763, South Korea

A surface-enhanced Raman scattering (SERS)-based gradient optofluidic sensor has been developed for a fast and sensitive immunoassay. In this work, a novel microfluidic sensor with functional internal structures has been designed and fabricated. This sensor is composed of three compartments consisting of the gradient channel that serially dilutes the target marker, the injection and mixing area of antibody-conjugated hollow gold nanospheres and magnetic beads, and the trapping area of sandwich immunocomplexes using multiple solenoids. Quantitative analysis of a specific target marker is performed by analyzing its characteristic SERS signals. This SERS-based gradient optofluidic sensor can replace the set of microwells or microtubes used in manual serial dilutions that have been traditionally used in enzyme-linked immunosorbent assay (ELISA)-type assays. The limit of detection for rabbit immunoglobulin (IgG) is estimated to be 1–10 ng/mL. This novel SERS-based optofluidic immunoassay system is expected to be a powerful clinical tool for the fast and sensitive medical diagnosis of a disease.

An immunoassay plays an important role in the fields of clinical diagnostics, drug discovery, food safety, and environmental monitoring.^{1–3} Traditionally, fluorescence-based detection systems have been widely used as a diagnostic tool for immunoassays, but this has several drawbacks including a poor limit of detection (LOD), photobleaching, and a limited multiplex detection capability.^{4–6} In particular, the LOD is an important issue in current immunoassay techniques because it is directly related to the potential capability for early disease diagnosis. Surface-enhanced Raman scattering (SERS)-based detection is considered

to be a promising technique for highly sensitive detection of a specific target marker.^{7–14} We recently reported a conceptually new SERS-based immunoassay technique using hollow gold nanospheres (HGNs) and magnetic beads.¹⁵ In that work, HGNs and magnetic beads were used as highly reproducible SERS probes and supporting substrates, respectively. The sandwich immunocomplexes were immobilized on the wall of a microtube using a small magnetic bar. Then, the quantitative analysis was performed by measuring the characteristic SERS signals of a Raman reporter. This SERS-based immunoassay overcomes the slow immunoreaction caused by the diffusion-limited kinetics on two-dimensional substrates because of the high surface-to-volume ratio of the magnetic beads. Consequently, the assay time was less than 1 h, including protein binding, washing, and optical detection steps. In addition, HGNs showed strong and reproducible enhancement effects from individual particles because hot spots can be localized on the pinholes on the hollow particle surface. For a well-known lung cancer marker, carcinoembryonic antigen (CEA), the LOD was estimated to be about 100–1000 times more sensitive than that of the fluorescence-based enzyme-linked immunosorbent assay (ELISA).

Nonetheless, a SERS-based immunoassay using microtubes and a magnetic bar still has some problems because it is awkward to optimize the experimental conditions such as the manual washing steps using a micropipet, changing the magnetic field intensity for an optimal SERS measurement and the inhomogeneous distribution of sandwich immunocomplexes immobilized on the wall of a microtube. In addition, various concentrations of a specific target marker should be manually prepared for its quantitative analysis. This time-consuming process makes the well plate- or microtube-based immunoassay less attractive.

* Corresponding author. E-mail: jbchoo@hanyang.ac.kr.

[†] Department of Bionano Engineering, Hanyang University.

[‡] Department of Mechanical Engineering, Hanyang University.

[§] College of Bionanotechnology, Kyungwon University.

[‡] Department of Biochemistry, Chungbuk National University.

- (1) Kanda, V.; Kariuki, J. K.; Harrison, D. J.; McDermott, M. T. *Anal. Chem.* **2004**, *76*, 7257–7262.
- (2) Terry, L. A.; White, S. F.; Tigwell, L. J. *J. Agric. Food Chem.* **2005**, *53*, 1309–1316.
- (3) Zangar, R. C.; Varnum, S. M.; Bollinger, N. *Drug Metab. Rev.* **2005**, *37*, 473–487.
- (4) Bally, M.; Halter, M.; Voros, J.; Grandin, H. M. *Surf. Interface Anal.* **2006**, *38*, 1442–1458.
- (5) Rosi, N. L.; Mirkin, C. A. *Chem. Rev.* **2005**, *105*, 1547–1562.
- (6) Peterson, A. W.; Heaton, R. J.; Georgiadis, R. J. *Am. Chem. Soc.* **2000**, *122*, 7837–7838.

- (7) Song, C. Y.; Wang, Z. Y.; Zhang, R. H.; Yang, J.; Tan, X. B.; Cui, Y. P. *Biosens. Bioelectron.* **2009**, *25*, 826–831.
- (8) Bao, F.; Yao, J. L.; Gu, R. A. *Langmuir* **2009**, *25*, 10782–10787.
- (9) Stevenson, R.; Ingram, A.; Leung, H.; McMillan, D. C.; Graham, D. *Analyst* **2009**, *134*, 842–844.
- (10) Sabatte, G.; Keir, R.; Lawlor, M.; Black, M.; Graham, D.; Smith, W. E. *Anal. Chem.* **2008**, *80*, 2351–2356.
- (11) Douglas, P.; Stokes, R. J.; Graham, D.; Smith, W. E. *Analyst* **2008**, *133*, 791–796.
- (12) Chen, J. W.; Lei, Y.; Liu, X. J.; Jiang, J. H.; Shen, G. L.; Yu, R. Q. *Anal. Bioanal. Chem.* **2008**, *392*, 187–193.
- (13) Li, T.; Guo, L. P.; Wang, Z. X. *Biosens. Bioelectron.* **2008**, *23*, 1125–1130.
- (14) Lin, C. C.; Yang, Y. M.; Chen, Y. F.; Yang, T. S.; Chang, H. C. *Biosens. Bioelectron.* **2008**, *24*, 178–183.
- (15) Chon, H.; Lee, S.; Son, S. W.; Oh, C. H.; Choo, J. *Anal. Chem.* **2009**, *81*, 3029–3034.

To resolve this problem, we have implemented our previously reported SERS immunoassay, performed in a microtube, into a microfluidic platform. Recently, SERS-based microfluidic sensors have been extensively applied for the highly sensitive analysis of many different types of chemical/biological targets.^{16–26} Here, a highly accurate and reproducible analysis is possible if a continuous flow and homogeneous mixing conditions are maintained in a microfluidic channel. In the present work, a gradient microfluidic channel^{27–32} to automatically achieve serial dilutions of a target marker has been fabricated. This device has been used to automatically dilute a target sample serially with buffer. For the formation of sandwich immunocomplexes in a microfluidic channel, the functionalized HGNs and magnetic beads with antibodies were introduced into the channel. Then, minisoloids were integrated into the microfluidic device for immobilization of the different concentrations of immunocomplexes. Here, minisoloids were placed close to each microfluidic channel to generate a magnetic field gradient to trap magnetic beads in a flowing stream. They can be switched on or off, and the field intensity can be tuned on demand. Finally, the SERS signal for the sandwich immunocomplexes immobilized on each microfluidic channel has been measured using a confocal Raman microscope. Consequently, a SERS-based immunoassay has been automatically performed in a microfluidic channel. With this novel technique, the tedious manual dilution process is eliminated and a fast and sensitive immunoanalysis has been achieved. Total assay time including incubation, detection, and washing steps was less than 30 min. To the best of our knowledge, this is the first report of a SERS-based optofluidic sensor using a gradient microfluidic channel integrated with solenoids for a fast and sensitive immunoassay.

EXPERIMENTAL SECTION

Preparation of Metal Nanoprobes and Antibody Conjugation. The preparation of HGNs and antibody conjugation onto metal nanoprobes has been reported elsewhere.^{33–35} Briefly, cobalt nanoparticles were synthesized by reducing CoCl_2 with NaBH_4 under N_2 gas purging conditions and were used as

templates for the HGNs. Here, gold atoms were nucleated and grown up to small shells around the cobalt template. Then, the cobalt was completely dissolved, and a hollow interior was formed. The wall thickness was controlled by changing the concentrations of HAuCl_4 . According to our transmission electron microscopy (TEM) measurements, the average diameter of the HGNs and the wall thickness were estimated to be 45 ± 12 and 15 ± 5 nm, respectively.

Conjugation of Raman reporters and antibodies was performed by the previously reported protocol.¹⁵ A Raman reporter, malachite green isothiocyanate (MGITC), was adsorbed onto the surface of the HGNs. MGITC ($1.0 \mu\text{L}$ of 5×10^{-5} M) was added to 1.0 mL of 0.7 nM HGNs, and the mixture was reacted for 2 h with stirring. The number of adsorbed MGITC molecules per particle is estimated to be approximately 72. Then, dihydrolipoic acid (DHLLA) was used for the antibody conjugation. The two $-\text{SH}$ terminal groups of DHLLA were cleaved and chemically bonded to the HGN surface. DHLLA ($2.0 \mu\text{L}$ of 5.0 mM) was added to 1 mL of 0.7 nM dye-adsorbed HGN and allowed to react for 1 h. The nonspecific sites remaining on the surface of the nanoparticle were coated with $2.0 \mu\text{L}$ of 2.5 mM mercaptoethanol. Excess nonspecific binding of mercaptoethanol in solution was removed by centrifuging the solution, and the precipitate was washed twice with phosphate buffered saline (PBS) buffer and resuspended using an ultrasonicator. As a result, nonspecific interactions of HGNs with other proteins as well as nanoparticle aggregations could be effectively prevented. For the activation of $-\text{COOH}$ terminal groups, $1.0 \mu\text{L}$ of 1.0 mM 1-ethyl-3-(3-dimethylaminopropyl) carbodiimide hydrochloride (EDC) and $1.0 \mu\text{L}$ of 1.0 mM *N*-hydroxysuccinimide (NHS) were added and allowed to react for 1 h. Carboxylate-terminated HGNs were used to achieve a stable immobilization of proteins by covalent bonding in the esterification of NHS with EDC.^{36–38} Finally, $1.0 \mu\text{L}$ of 10 μM polyclonal antirabbit IgG (excess amount) was added to NHS-activated HGNs and reacted overnight at 4 °C. Here, antibody immobilization onto the HGNs occurs by displacement of the NHS group by the lysine residues of the antibody. Unreacted NHS groups on the surface of the HGNs were deactivated with $1.0 \mu\text{L}$ of 1 mM ethanolamine for 2 h. Nonspecific binding chemicals and antibodies were removed by centrifuging, and the final nanoprobes were washed twice with PBS buffer.

For the activation of other $-\text{COOH}$ terminal groups on the magnetic beads, $10 \mu\text{L}$ of 3.0 mM NHS and $10 \mu\text{L}$ of 3.0 mM EDC were added to 1.0 mL of 0.5 mg/mL magnetic beads and allowed to react for 1 h. Then, $1.0 \mu\text{L}$ of 1 mM monoclonal antirabbit IgG (excess amount) was added to NHS-activated magnetic beads and

- (16) Park, T.; Lee, S.; Seong, G. H.; Choo, J.; Lee, E. K.; Kim, Y. S.; Ji, W. H.; Hwang, S. Y.; Gweon, D. G.; Lee, S. *Lab Chip* **2005**, *5*, 437–442.
- (17) Yea, K.; Lee, S.; Kyong, J. B.; Choo, J.; Lee, E. K.; Joo, S. W.; Lee, S. *Analyst* **2005**, *130*, 1009–1011.
- (18) Lee, D.; Lee, S.; Seong, G. H.; Choo, J.; Lee, E. K.; Gweon, D. G.; Lee, S. *Appl. Spectrosc.* **2006**, *60*, 373–377.
- (19) Chen, L. X.; Choo, J. B. *Electrophoresis* **2008**, *29*, 1815–1828.
- (20) Quang, L. X.; Lim, C.; Seong, G. H.; Choo, J.; Do, K. J.; Yoo, S. K. *Lab Chip* **2008**, *8*, 2214–2219.
- (21) Wang, G.; Lim, C.; Chen, L.; Chon, H.; Choo, J.; Hong, J.; deMello, A. J. *Anal. Bioanal. Chem.* **2009**, *394*, 1827–1832.
- (22) Lee, S.; Choi, J.; Chen, L.; Park, B.; Kyong, J. B.; Seong, G. H.; Choo, J.; Lee, Y.; Shin, K. H.; Lee, E. K.; Joo, S. W.; Lee, K. H. *Anal. Chim. Acta* **2007**, *590*, 139–144.
- (23) Tong, L.; Righini, M.; Gonzalez, M. U.; Quidant, R.; Käll, M. *Lab Chip* **2009**, *9*, 193–195.
- (24) Keir, R.; Igata, E.; Arundell, M.; Smith, W. E.; Graham, D.; McHugh, C.; Cooper, J. M. *Anal. Chem.* **2002**, *74*, 1503–1508.
- (25) Wilson, R.; Monaghan, P.; Bowden, S. A.; Parnell, J.; Cooper, J. M. *Anal. Chem.* **2007**, *79*, 7036–7041.
- (26) Wilson, R.; Bowden, S. A.; Parnell, J.; Cooper, J. M. *Anal. Chem.* **2010**, *82*, 2119–2123.
- (27) Dertinger, S. K. W.; Chiu, D. T.; Jeon, N. L.; Whitesides, G. M. *Anal. Chem.* **2001**, *73*, 1240–1246.
- (28) Jiang, X. Y.; Ng, J. M. K.; Stroock, A. D.; Dertinger, S. K. W.; Whitesides, G. M. *J. Am. Chem. Soc.* **2003**, *125*, 5294–5295.
- (29) Herrmann, M.; Veres, T.; Tabrizian, M. *Lab Chip* **2006**, *6*, 555–560.
- (30) Stroock, A. D.; Dertinger, S. K.; Ajdari, A.; Mezic, I.; Stone, H. A.; Whitesides, G. M. *Science* **2002**, *295*, 647–51.

- (31) deMello, A. J. *Nature* **2006**, *442*, 394–402.
- (32) Chen, L.; Wang, G.; Lim, C.; Seong, G. H.; Choo, J.; Lee, E. K.; Kang, S. H.; Song, J. M. *Microfluid. Nanofluid.* **2009**, *7*, 267–273.
- (33) Lee, S.; Chon, H.; Lee, M.; Choo, J.; Shin, S. Y.; Lee, Y. H.; Rhyu, I. J.; Son, S. W.; Oh, C. H. *Biosens. Bioelectron.* **2009**, *24*, 2260–2263.
- (34) Schwartzberg, A. M.; Oshiro, T. Y.; Zhang, J. Z.; Huser, T.; Talley, C. E. *Anal. Chem.* **2006**, *78*, 4732–4736.
- (35) Wang, H.; Goodrich, G. P.; Tam, F.; Oubre, C.; Nordlander, P.; Halas, N. J. *J. Phys. Chem. B* **2005**, *109*, 11083–11087.
- (36) Hibbert, D. B.; Gooding, J. J.; Erokhin, P. *Langmuir* **2002**, *18*, 1770–1776.
- (37) Gooding, J. J.; Praig, V. G.; Hall, E. A. H. *Anal. Chem.* **1998**, *70*, 2396–2402.
- (38) Park, T.; Choo, J.; Lee, M.; Kim, Y. S.; Lee, E. K.; Lee, H. S. *Anal. Sci.* **2004**, *20*, 1255–1258.

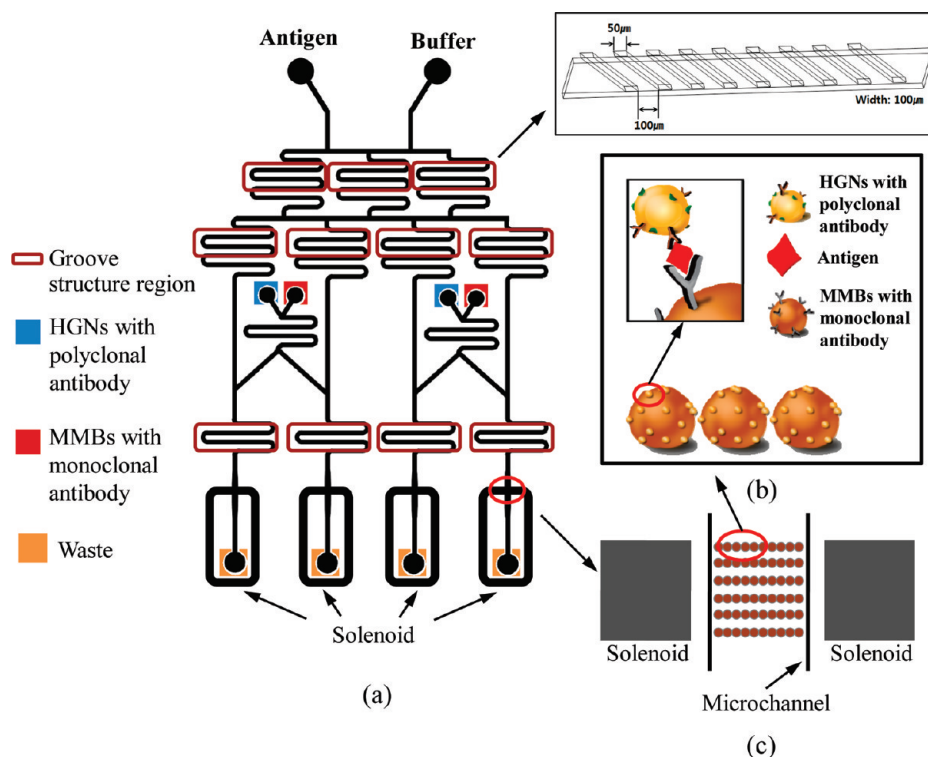


Figure 1. (a) Layout of SERS-based gradient optofluidic sensor integrated with solenoids. (b) Formation of sandwich immunocomplex between HGNs and magnetic beads. (c) Trapping of sandwich immunocomplexes in a microfluidic channel.

reacted overnight. Here, unreacted antibodies were washed out using a micropipet after immobilization of the magnetic beads by use of a magnetic bar. Unreacted NHS groups on the surface of the magnetic beads were also deactivated with 10 μ L of 3.0 mM ethanolamine for 2 h. Nonspecific binding chemicals and antibodies were removed by centrifuging, and the final nanoprobe were washed twice with PBS buffer.

Fabrication of a Gradient Microfluidic Channel Integrated with Minisolenoids. A three-step procedure was adopted to fabricate the gradient microfluidic device: polydimethylsiloxane (PDMS) replica fabrication, placement of solenoids in the PDMS channel, and sealing of the chip to a slide glass.³⁹ The gradient microfluidic device was fabricated by soft lithography and rapid prototyping with PDMS technology. As shown in Figure 1, the pattern including groove mixers was transferred to a 4 in. silicon wafer through a high-resolution photomask (AutoCAD 2008/Auto Desk Inc., OR, USA). Sylgrad 184 PDMS prepolymer was thoroughly mixed with its curing agent at 10:1 (v/v) and then degassed using a vacuum pump. Here, a groove-shaped mixer was incorporated into the channel to improve its mixing efficiency. As the confluent streams travel along the channel, they were repeatedly split and combined at the nodes with neighboring streams and then allowed to mix by diffusion in the serpentine region.

Afterward, four handmade yoke-type solenoids were placed at positions around the channel outlets. Each solenoid was prepared by coiling 26 turns of copper wire (insulated with lacquer on the surface, 0.45 mm in diameter) on the ferroelectric yoke with dimensions of 1 mm diameter, 9 mm height, 4 mm width, and 1 mm gap between the channels. These solenoids generate suf-

ficient magnetic field to trap the magnetic beads. For optimal magnetic field generation, the relationship between the direct current and the induced magnetic field was considered. The induced magnetic field has a linear relationship with the current, and 27 mT of magnetic field intensity was obtained when 2 A of direct current was applied to the coils. This field intensity was evaluated to be optimum for on-chip immunoassay measurements. To find this value, both the current and magnetic field intensities have been varied by changing the number of coil turns.

After curing at 75 $^{\circ}$ C for 2 h, the solidified PDMS was peeled off from the master and access holes were punched. Finally, the PDMS block was bonded permanently onto a glass substrate using oxygen plasma treatment. The oxidation of PDMS results in a hydroxyl-terminated surface which promotes adhesion. To achieve bonding between a PDMS block and a glass substrate, two plasma-treated substrates are brought into conformal contact. This treatment produces an irreversible seal at their interface through the formation of Si–O–Si bonds.⁴⁰

SERS Signal Measurements. Renishaw 2000 Raman spectrometers were used with Melles Griot He–Ne 633 nm laser irradiation. The Rayleigh line was removed from the collected Raman scattering using a holographic notch filter located in the collection path. Each spectrometer was calibrated daily, prior to any spectral collection, through measuring the position of the silicon reference peak at 520.01 cm^{-1} and making an offset correction whenever necessary. For 633 nm, laser radiation spectra were collected via an extended scan in the region of 1700–700 cm^{-1} , with a laser power of 30 mW. A collection time of 10 s and a 20 \times objective lens was used to focus the laser spot. Raman scattering was collected using a charge-coupled

(39) Liu, Y. J.; Guo, S. S.; Zhang, Z. L.; Huang, W. H.; Baigl, D. M.; Chen, Y.; Pang, D. W. *J. Appl. Phys.* **2007**, *102*, 084911.

(40) Patrito, N.; McLachlan, J. M.; Faria, S. N.; Chan, J.; Norton, P. R. *Lab Chip* **2007**, *7*, 1813–1818.

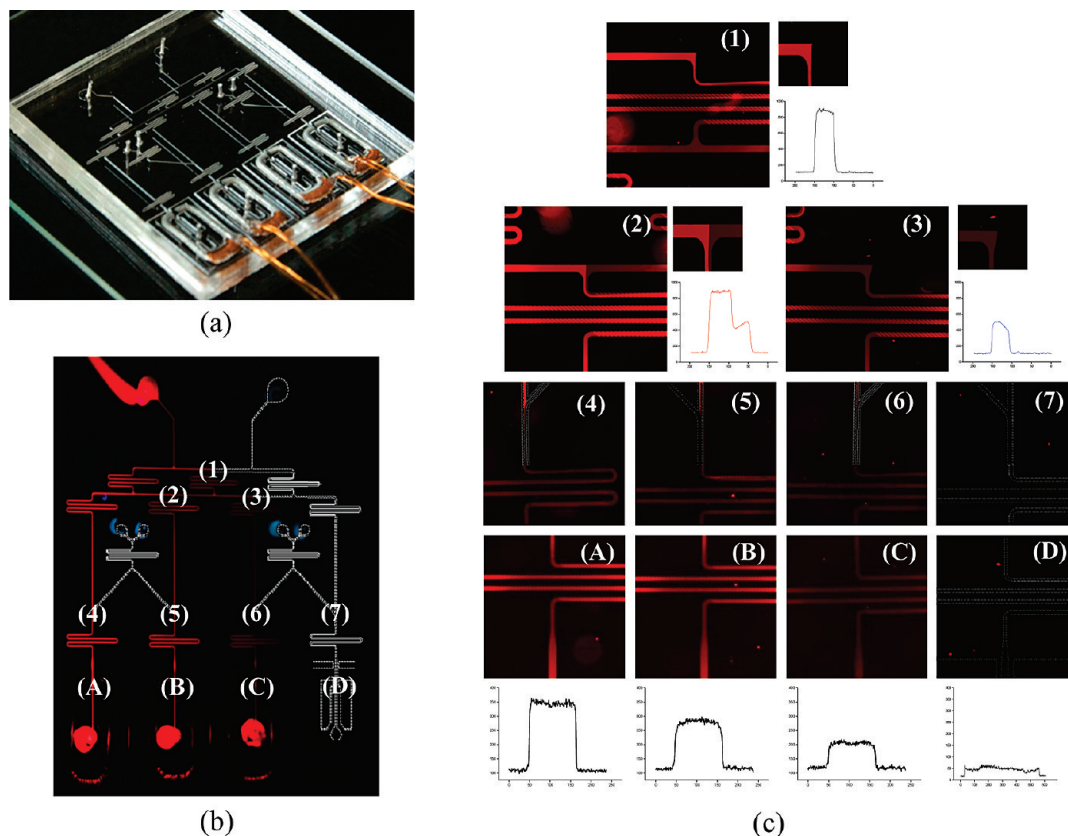


Figure 2. (a) Photograph and (b) layout of SERS-based gradient optofluidic sensor integrated with solenoids. (c) Amplified images of each branching point. Graphs indicate the measured fluorescent intensity profiles across the channel.

device (CCD) camera at a spectral resolution of 4 cm^{-1} . An additional CCD camera was fitted to an optical microscope to obtain optical images. All the spectral data were treated with the GRAMS software. The baseline was adjusted by two point level baseline correction at 750 and 1720 cm^{-1} after the smoothing process using a binomial smoothing algorithm.

RESULTS AND DISCUSSION

Recently, we reported a quick and reproducible SERS-based immunoassay technique using HGNs and magnetic beads in a microtube.¹⁵ In that technique, various concentrations of marker solution should be prepared prior to its quantitative analysis. This process is time-consuming and sometimes leads to serious experimental errors during the preparation of different concentrations of target samples. To resolve the problems in our previous report, a SERS-based optofluidic sensor using a gradient channel integrated with solenoids was developed in this work. Herein, various concentrations of antigen solutions can be automatically generated using a network of gradient channels. As previously reported by Dertinger et al.²⁷ the branching structure of the channel serially dilutes one stream with a second stream. Consequently, the laminar flow of fluids inside the channel permits multiple streams of solutions containing different concentrations of flow side by side. By adjusting the chemical compositions of individual streams, various concentration profiles can be generated. The technique replaces the set of microtubes or microwells used for manual serial dilutions in the previous report.¹⁵

Figure 1a shows a schematic layout of the gradient microfluidic channel integrated with four minisolenoids. This channel is

composed of three compartments. The first compartment is the gradient channel that serially dilutes the antigen marker using a network of channels. This part automatically generates a series of different concentrations of solution by continuously mixing and diluting the antigen with a buffer solution. The second compartment is the injection and mixing part for the magnetic beads and HGNs for the formation of the sandwich immunocomplexes. Here, both the magnetic beads and HGNs were introduced into the channel, and they were mixed with different concentrations of antigen targets under flow conditions. As mentioned above, a groove-shaped mixer was incorporated into the channel to improve the mixing efficiency, as shown in Figure 1. Consequently, sandwich immunocomplexes were produced as shown in Figure 1b by antibody–antigen–antibody interactions. The final compartment is the trapping and detection part for the sandwich immunocomplexes. To achieve fast and efficient trapping of the magnetic beads in the flowing stream, two minisolenoids were arranged at the end part of each channel, as shown in Figure 1c. After trapping the immunocomplexes, the SERS signal was measured by focusing the laser beam on each microfluidic channel.

To evaluate the mixing efficiency and the capability of generating accurate concentrations of a marker in the gradient microfluidic channel, fluorescence measurements using a confocal microscope have been performed. Figure 2 demonstrates the result of a mixing test using red quantum dots (QD: 655 nm fluorescence emission). In this work, the rabbit IgG was used as a target antigen. To find the optimum flow rate for the fluorescence measurements, the flow rate was varied from 0.1 to $2.0\text{ }\mu\text{L}/$

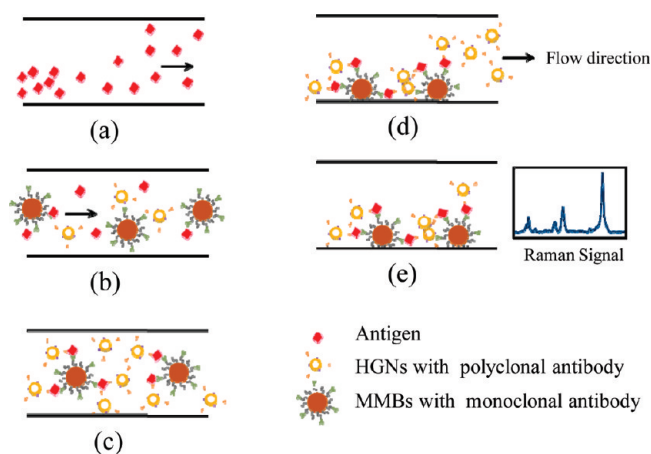


Figure 3. Schematic representation for the procedure of the on-chip immunoassay in a microfluidic channel: (a) generation of various concentrations of a target marker; (b) introduction of antibody-conjugated HGN probes and magnetic beads; (c) formation of sandwich immunocomplexes; (d) immobilization using solenoids, 10 min incubation, and washing; (e) SERS detection for sandwich immunocomplexes. Total assay time is about 30 min from serial dilution to SERS detection.

min by regulating the microsyringe pump. According to our experimental data, the flow rate conditions of $1.0 \mu\text{L}/\text{min}$ (for rabbit IgG antigen and 0.05% PBS buffer) and $1.5 \mu\text{L}/\text{min}$ (for HGNs and magnetic beads) were evaluated to be optimal for the generation of a stable laminar flow at each branching point (1–7 in Figure 2c). As the confluent streams travel along the channel, they were repeatedly split at the nodes, combined with neighboring streams, and allowed to mix by diffusion in the serpentine region. Here, groove-shaped mixers were incorporated into all of the channels to improve the mixing efficiency. Consequently, the fluorescence intensity gradually decreased from left to right along with the decrease in the antigen concentration. The fluorescence profiles from (A) to (D) on the bottom of Figure 2c show the corresponding fluorescence intensity changes across each channel. The fluorescence intensities in each channel were estimated to be (A) 100%, (B) 80%, (C) 40%, and (D) 0%. Using this gradient microfluidic device, it is possible to automatically generate a series of solutions containing exponentially decreasing concentrations of antigens.²⁷ This design achieves 1:1 mixing of antigen and buffer in each stage of dilution. Thus, each stage decreases the concentration of antigens by one-half.

Figure 3 shows a schematic representation of the experimental protocol for an on-chip immunoassay. A sandwich-type immunoassay of rabbit IgG using SERS detection was performed through the following steps. (a) Various concentrations of rabbit IgG antigen were generated using a gradient microfluidic device. (b) Polyclonal antibody-conjugated HGNs and monoclonal antibody-conjugated magnetic beads were introduced into the channel and mixed with different concentrations of antigens in the flow. (c) Sandwich immunocomplexes were formed in each channel. (d) Immunocomplexes were immobilized inside the channel by applying magnetic fields and were incubated for 10 min. Then, they were washed with buffer solution to remove nonspecific binding antigens, magnetic beads, and HGNs. (e) SERS signals were measured for the immobilized immunocomplexes in each channel.

As shown in Figure 1, four minisolenoid sets were placed in the side parts of each channel for the efficient magnetic trapping of sandwich immunocomplexes inside the channel. To achieve an optimal magnetic field generation, the relation between the direct current and the induced magnetic field was considered. Here, the induced magnetic field has a linear relationship with the current. Twenty-seven millitesla of magnetic field intensity was obtained when 2 A of direct current was applied to the coils, and this was estimated to be the optimal magnetic field intensity for reproducible SERS measurements. Figure 4 shows the optimal magnetic bead-capturing conditions for four parallel channels under the optimal magnetic field. Before applying the current, all of the magnetic streams are dispersed inside the channel and no capturing occurred. When the solenoids were turned on, magnetic fields were induced around the channel walls and the magnetic beads started to be trapped in the channel. To collect enough magnetic beads for SERS signal measurements, they were accumulated and incubated for 10 min. Then, they were washed with buffer solution. Finally, the syringe pump was stopped, and the SERS signals were measured under the steady-state condition by moving the laser spot to each channel.

SERS signal intensities of Raman reporter (MGITC) molecules, adsorbed onto the surface of HGNs, are dominant over those measured from other chemical constituents or antibodies. When the SERS spectra for MGITC-labeled HGNs alone and sandwich immunocomplexes were compared with each other, only the SERS signals from MGITC were observed in all the spectra. This means that the SERS intensity of MGITC is much stronger than others, and its variation can be used as the quantitative indicator of antigen marker.

To generate seven different concentrations of the rabbit IgG antigen, two gradient microfluidic devices have been used. Figure 5a shows the SERS spectra collected from sandwich immunocomplexes in each microfluidic channel. In absence of IgG antigen, a weak SERS signal was observed (0 ng/mL). This indicates that a small amount of HGNs still remained in the solution by nonspecific binding, even though most of HGNs were removed from the solution by washing. However, this factor was considered in its calibration process. The intensity of the Raman peaks increases concomitantly with the increase in the concentration of the antigen. Here, the Raman peak centered at 1616 cm^{-1} was used for quantitative evaluation of the antigen. The calibration curve is shown in Figure 5b, where the error bars indicate standard deviations from four measurements. A good linear response was achieved within the concentration range from 0 to 100 ng/mL. This means that highly sensitive and reproducible immunoassays in a microfluidic channel are possible using this SERS-based optofluidic sensor integrated with solenoids. In particular, the tedious manual process of serial dilutions can be avoided by applying the gradient micronetwork channels. Moreover, the assay time was greatly reduced compared with traditional ELISA-based assays because of the high surface-to-volume ratio of the magnetic beads.

CONCLUSION

In the present study, a SERS-based optofluidic system for fast and sensitive immunoassay has been developed. The microfluidic channel used here is composed of three compartments: the gradient channel that serially dilutes the target marker, the

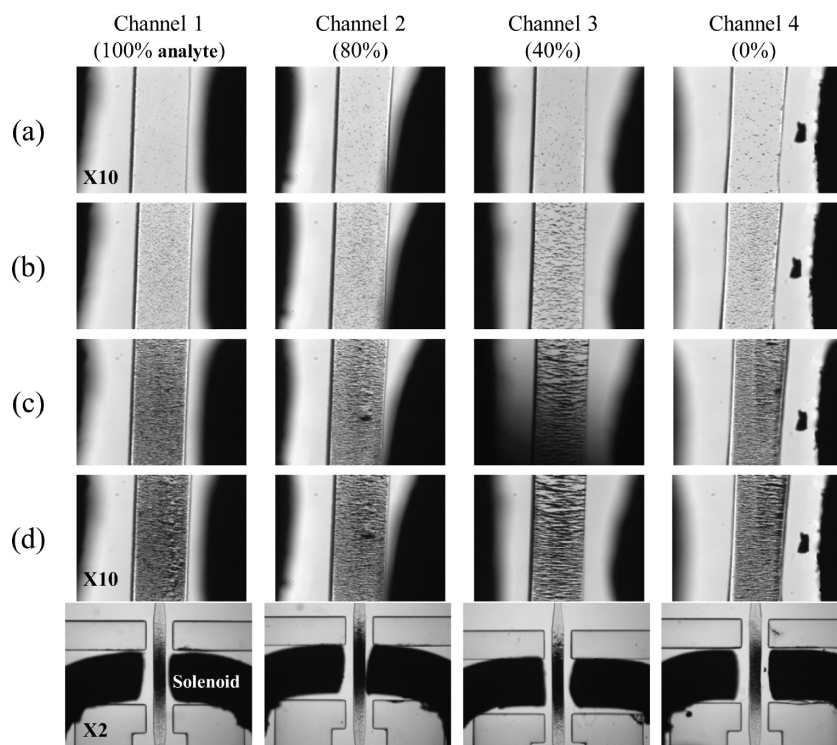


Figure 4. Microscopic photographs for the trapped immunocomplexes in the channel: (a) before applying the current (solenoid off), (b) after applying the current (solenoid on), (c) 10 min after, and (d) under steady-state condition.

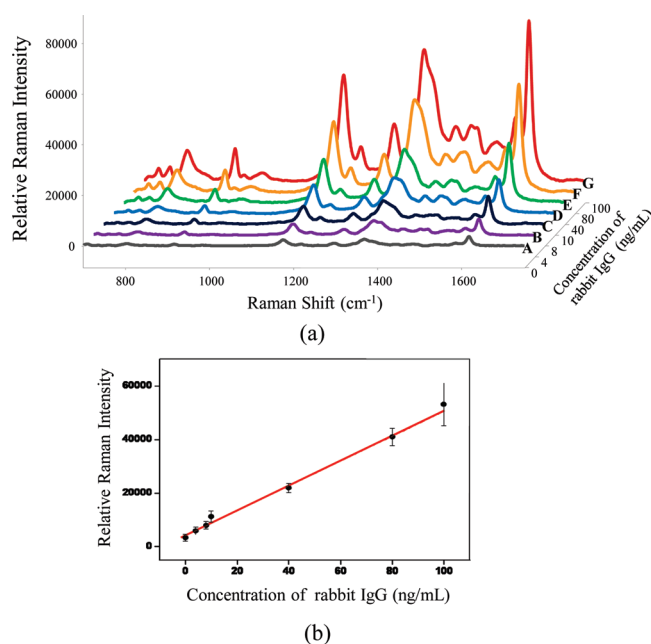


Figure 5. (a) SERS spectra for decreasing concentrations of rabbit IgG: (A) 0 ng/mL, (B) 4 ng/mL, (C) 8 ng/mL, (D) 10 ng/mL, (E) 40 ng/mL, (F) 80 ng/mL, and (G) 100 ng/mL. (b) Corresponding intensity change of the SERS signal at 1616 cm^{-1} . It shows a linear relationship over the whole concentration range from 0 to 100 ng/mL (coefficient of determination, $R^2 = 0.988$). Error bars indicate standard deviations from four measurements.

injection and mixing part of magnetic beads and HGNs, and the trapping part of the sandwich immunocomplexes using multiple solenoids. The potential immunoanalytical capability of this system has been evaluated for various concentrations of rabbit IgG antigen. Here, different concentrations of IgG antigen could be

automatically generated by the gradient channel, and the sandwich immunocomplexes were successfully trapped by multiple solenoids. Quantitative analysis has been performed by measuring the SERS signal at 1616 cm^{-1} . A good linear response was obtained in the concentration range from 0 to 100 ng/mL. The LOD for rabbit IgG antigen has been estimated to be 1–10 ng/mL from the standard deviations above the background. Our proposed SERS-based optofluidic immunoassay system, using antibody-conjugated HGNs and magnetic beads, has several advantages over other previously reported SERS immunoassays performed in microwells or microtubes. The tedious manual dilution process is eliminated because various concentrations of target marker are automatically generated by a network gradient channel. The assay time from serial dilution to SERS detection takes less than 30 min because all of the experimental conditions for the formation, immobilization, and detection of immunocomplexes are automatically controlled inside the exquisitely designed microfluidic channel. Thus, this novel SERS-based optofluidic assay technique is expected to be a powerful clinical tool for fast and sensitive disease diagnosis. The simultaneous detection of three target cancer markers in clinical serum, obtained from the University Hospital, is under investigation using this technology.

ACKNOWLEDGMENT

This work was supported by the National Research Foundation of Korea (Grant Numbers R11-2010-044-1001-0 and K20904000004-09A0500-00410).

Received for review March 23, 2010. Accepted May 17, 2010.

AC100736T